Reprinted from the Preprint Volume of the Eighth Conference on Atmospheric and Oceanic Waves and Stability, October 14-18, 1991, Denver, Colo. Published by the American Meteorological Society, Boston, Mass.

P1.16

ENERGY SOURCE FOR INHOMOGENEOUS TURBULENCE ON A ROTATING SPHERE

H. L. Tanaka

Geophysical Institute
University of Alaska Fairbanks
Fairbanks, Alaska

1. Introduction

Large-scale atmospheric energy cascades from source ranges to dissipation ranges through wave-wave interactions or turbulence. Kraichnan (1967) and Leith (1968) showed that inertial energy transfers in two-dimensional (2-D) isotropic turbulence allow two equilibrium states: the -5/3 and -3 power law inertial subranges. Recently, Lilly (1989) discussed the possibility of four inertial subranges for the case of two separate variance sources. These include a large planetary-scale -5/3 range, a small synoptic-scale -3 range with a down-scale enstrophy cascade, a mesoscale -5/3 range with an up-scale 2-D kinetic energy cascade, and a micro-scale isotropic -5/3 range with a down-scale 3-D kinetic energy cascade. This suggests that both the -3 and -5/3 power laws of the 2-D inertial subrange exist in planetary-scale motions. The planetary-scale -5/3 power law is, however, not confirmed yet from observations.

According to the normal mode energetics analysis (e.g., Tanaka 1985; Tanaka and Kung 1988) the energy spectrum of the real atmosphere projected onto three-dimensional normal mode functions (3-D NMFs) exhibits a clear, single spectral peak in the eigenfrequency domain. Here eigenfrequencies of Laplace's tidal equations for various equivalent heights are considered to represent the 3-D scale of the NMFs due to the intrinsic dispersion relation of Rossby waves. The energy peak separates the region of a 3 power law in the low-frequency range of Rossby modes and the -5/3 power law in the high-frequency range of gravity modes. Interestingly, the spectral slope of the largest-scale Rossby modes obeys the -5/3 law and merges with the gravity modes' -5/3 law. The peak is therefore not merely associated with the largest-scale motions, but it occurs in the intermediate scale. The largest-scale -5/3 range in the eigenfrequency domain appears to agree with Lilly's prediction by 2-D turbulence.

The interpretation of the distinct energy peak in the intermediate range of the eigenfrequency domain is an open question. For synoptic disturbances the energy peak may result from atmospheric baroclinic instability, because the growth rates of the unstable modes are large (e.g., Young and Villere, 1985; Tanaka and Kung, 1989). For planetary waves, however, there is no clear interpretation of the spectral peak and the evident 3 and -5/3 power law in the eigenfrequency domain. The energy source and wave saturation processes for large-scale motions need to be studied and explained.

The purpose of this study is to evaluate energy and energy-source spectra in the 3-D spectral domain resulting from atmospheric baroclinic instability. Baroclinic instability on a sphere is examined for a monthly-mean basic state of January 1979, using the 3-D spectral primitive equations with the basis of vertical structure functions and Hough harmonics, as derived by Tanaka and Kung (1989). For comparison, the observed energy spectra based on the analysis of normal mode energetics during the First GARP Global Experiments (FGGE) were reproduced (Tanaka, 1985; Tanaka and Kung, 1988). It will be shown that the energy source due to baroclinic instability coincides with the observed energy peaks in the eigenfrequency domain both for synoptic and planetary waves.

2. Governing equations

Using a three-dimensional spectral representation, a system of primitive equations in a spherical coordinate may be written as:

$$\frac{dw_i}{d\tau} + i\sigma_i w_i = -i \sum_{j=1}^{M} \sum_{k=1}^{M} r_{ijk} w_j w_k + f_i, \quad i = 1, 2, \ldots, M, \quad (1)$$

where w_i and f_i are the Fourier expansion coefficients of dependent variables and diabatic processes, σ_i are Laplace's tidal frequencies, r_{ijk} are interaction coefficients, and M is the total number of the series expansion for the 3-D atmospheric variables. Refer to Tanaka and Sun (1990) for the details. The expansion basis functions consist of vertical normal modes and Hough harmonics. The Hough harmonics comprise rotational (Rossby) modes and westward and eastward propagating gravity modes. They are distinguished by different meridional indices l_R, l_W, and l_E, respectively.

The nonlinear equation (1) is linearized for the prescribed basic state, using notations $\overline{w}_i$ and $\overline{f}_i$ for the time-independent zonal basic state and w_i' and f_i' for small perturbations superimposed on the basic state. The resulting system of linear equations for the first-order terms of the

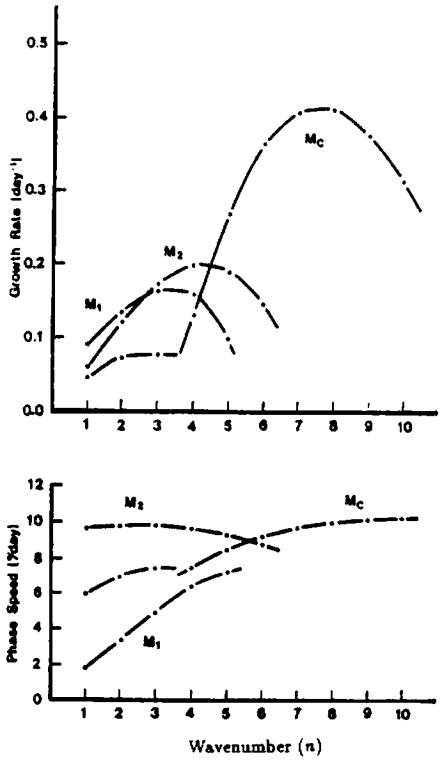

Fig. 1. Growth rates and phase speeds of the shallow Charney modes, M_C, dipole Charney modes M_2 and slow Charney modes M_1

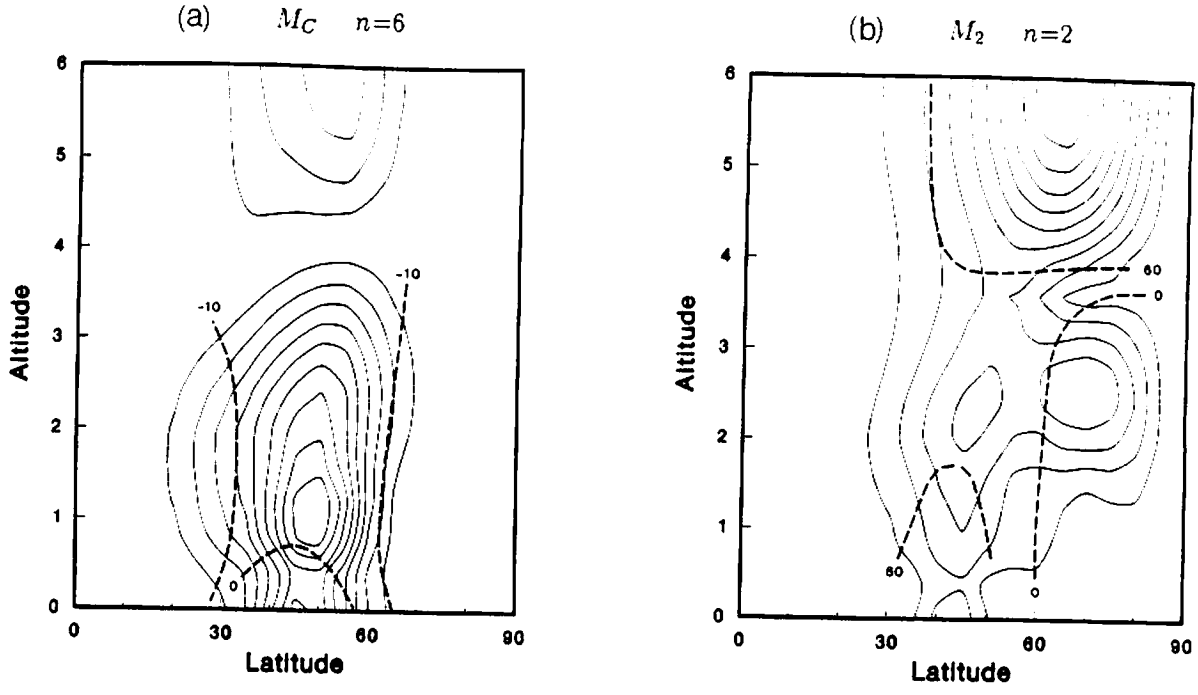

Fig. 2. Meridional-height cross sections of the geopotential amplitude and phase for (a) M_C of n=6 and (b) M_2 of n=2.

perturbation quantities can be expressed in a matrix form. For inviscid and adiabatic perturbations, it becomes

$$\frac{d}{d\tau}W + iDW = -iBW, \qquad (2)$$

where W is a variable vector consisting of w_i', D is a diagonal matrix of σ_i, and the (i,j) entry of the real matrix B is determined by the expansion coefficients of $\overline{w}_i$. The real and imaginary parts of the eigenvalue for the eigenvalue problem of a real matrix $(D+B)$ give the frequency and growth rate. By solving (2) for the prescribed zonal basic state, we can examine the unstable modes which provide the energy source for synoptic and planetary waves.

Figure 1 illustrates the growth rates and phase speeds analyzed from a realistic zonal basic state of the monthly mean for January 1979 (after Tanaka and Kung, 1989). There is a dominant unstable mode in synoptic waves with a maximum growth rate of 0.4 (1/day) (e-folding time is approximately 2.5 day) and a phase speed of 10 (°/day). This unstable mode is identified as a shallow Charney mode, M_C, on a sphere. Different types of unstable modes, M_1 and M_2, dominate at planetary waves. The most unstable modes at zonal wavenumber n=3-4, M_2, are identified as a dipole Charney mode (a Charney mode, but with a meridional dipole structure as in Fig. 2). The most unstable mode at n=1-2, M_1, is referred to as a slow Charney mode due to the characteristics of the slow phase speed. To understand the vertical and meridional energy spectrum in the following, a meridional-height cross-section of the geopotential field is given in Fig. 2 for M_C of n=6 and for M_2 of n=2.

3. Results of the energy spectrum

Atmospheric energy spectra in the vertical wavenumber domain (inverse of an equivalent height h_m^{-1}) are illustrated in Fig. 3a for zonal wavenumbers n= 6. The subscript m denotes a vertical index. The Rossby modes indicate energy peaks at $h_m^{-1} = 1 \times 10^{-4}$ and 7×10^{-3} with a weak peak at $h_m^{-1} = 5 \times 10^{-2}$. The energy levels decrease rapidly in the higher vertical modes beyond $h_m^{-1} = 7 \times 10^{-3}$. On the other hand, gravity mode energy distributions indicate peaks at $h_m^{-1} = 7 \times 10^{-3}$. The energy levels are two orders of magnitude lower than that of Rossby modes for the barotropic component, whereas these become comparable near $h_m^{-1} = 1 \times 10^{-1}$.

The eigenfrequency σ_{nlm} given in (1) describes the meridional scale of the mode within the same type of Rossby and gravity modes for the fixed n and m. The larger the meridional index, the smaller the modal meridional scale. As the meridional index increases, the magnitude of the eigenfrequency $|\sigma_{nlm}|$ decreases monotonically within Rossby modes; whereas it increases monotonically within gravity modes. Consequently, the discrete spectrum of $|\sigma_{nlm}|$ spans the entire positive frequency domain. Mixed Rossby-gravity modes (l_R=0) and Kelvin modes (l_E=0) are positioned at the boundary of the Rossby and gravity modes. The spectral characteristics, such as the power law in the wavenumber domain, are transformed to the frequency domain.

The results of atmospheric energy spectra as functions of $|\sigma_{nlm}|$ are illustrated in Fig. 3b for n= 6. The three panels in each figure describe the energy spectra of the vertical indices of m=0, 2, and 4, corresponding to $h_m^{-1} = 1 \times 10^{-4}$, 2×10^{-3} and 7×10^{-3}, respectively. A clear energy peak is seen at $|\sigma_{nlm}| = 8 \times 10^{-2}$ for m=0, at 6×10^{-2} for m=2, and at 2×10^{-2} for m=4. A red shift appears in the energy peaks for the higher vertical modes. The spectral slopes in the low-frequency range are less steep than the 3 power law in m=0 and 2, but the slope is steeper than 3 in m=4. The slopes in the high-frequency range are about -5/3 for m=0, and these are less steep for m=2 and 4. The spectral characteristics of n=4 and 2 (not shown) are very similar to those for n=6.

Evidently, the energy peaks are not merely associated with the largest-scale Rossby and gravity modes, but the peaks occur at the intermediate meridional scale of the Rossby modes. We have demonstrated that the characteristic bimodal energy peaks found in Fig 3a and the distinct energy peaks in Fig. 3b become clearer in the transient components of atmospheric motions. Therefore, the spectral peaks are more associated with the transient motions of the atmosphere.

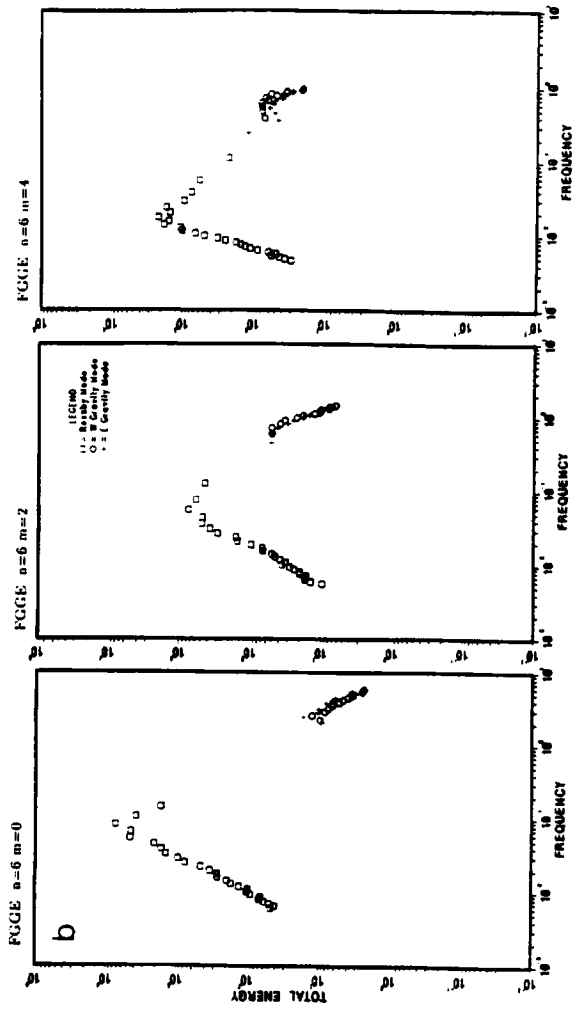

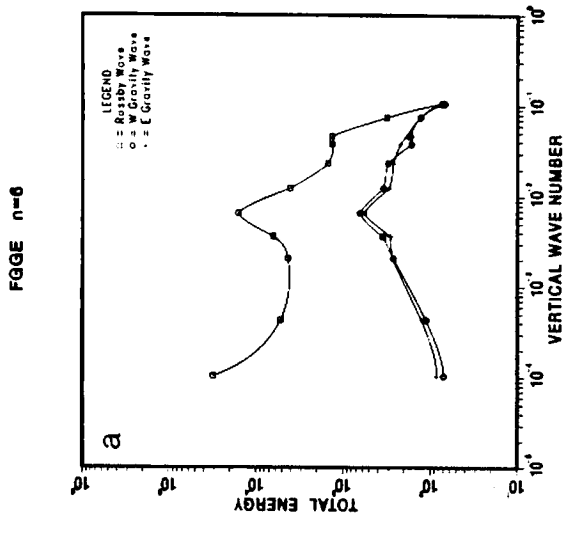

Fig. 3. Spectral distributions of atmospheric total energy (a) in the vertical wavenumber domain and (b) in the eigenfrequency domain for n= 6 during the FGGE winter.

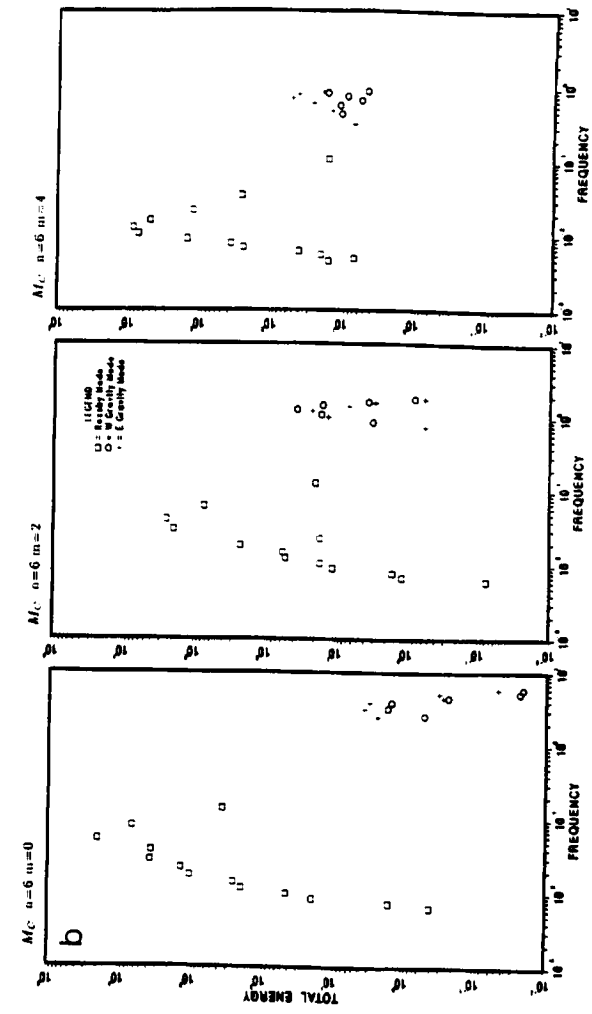

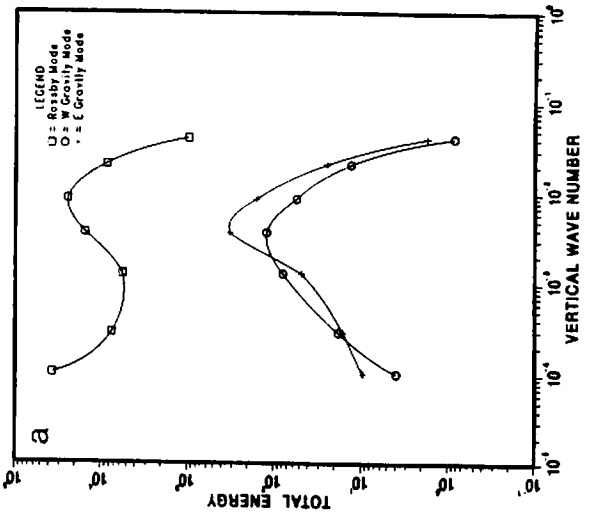

Fig. 4. As in Fig. 3 but for the shallow Charney mode M_C for n= 6. The three panels in each figure represent the vertical indices m=0, 2, and 4.

The energy spectrum in the vertical wavenumber domain for the most unstable mode at n=6 is illustrated in Fig. 4a, using the same format as presented in Fig. 3a. The spectrum indicates bimodal peaks at $h_m^{-1} = 1 \times 10^{-4}$ and 9×10^{-3}. There is an evident energy gap at $h_m^{-1} = 1 \times 10^{-3}$. The energy levels drop rapidly for the larger vertical wavenumbers. Spectral characteristics coincide with the observations shown in Fig. 3a. Energy peaks in gravity modes are seen at $h_m^{-1} = 4 \times 10^{-3}$, also coinciding with observations. Hence, it is reasonable to interpret that the observed bimodality in the vertical energy spectrum for n=6 is the result of atmospheric baroclinic instability of the shallow Charney mode.

Figure 4b illustrates the energy spectrum in the eigenfrequency domain for the most unstable mode at n=6. The unstable mode exhibits evident spectral peaks at $|\sigma_{nlm}| = 6 \times 10^{-2}$ for m=0, at 4×10^{-2} for m=2, and at 1×10^{-2} for m=4. These spectral peaks coincide fairly well with the observations shown in Fig. 3b. Secondary energy peaks appear in the high-frequency range. The characteristic red shift of the major peaks for the larger vertical wavenumbers is detected as it was in the observed energy spectrum. Considering the fact that the energy source has a spectral shape identical to the energy spectrum, we confirm that the observed energy peaks in the frequency domain are produced by the energy source resulting from atmospheric baroclinic instability. The present linear model, however, cannot explain the observed power law due to the lack of nonlinear interactions. In the real atmosphere, the supplied energy in the source range would cascade away to the rest of the frequency domain by nonlinear scattering. This finding may suggest an interpretation of atmospheric large-scale disturbances from the standpoint of inhomogeneous turbulence by Shepherd (1987) that results in energy transfer between different meridional scales along a constant zonal wavenumber.

Finally, we compared the energy spectra of the slow Charney mode and the dipole Charney mode at n=4 and 2 (not shown). These two unstable modes show similar energy spectra, indicating the bimodal vertical energy peaks as previously seen. The bimodality appears to be a common feature in all Charney-type baroclinic instability. The energy levels of the gravity modes are negligible, which justifies the use of the quasi-geostrophic theory for these two modes. For the energy spectra in the eigenfrequency domain, energy spectra of these two Charney modes exhibit essentially the same energy peaks and both are similar to observations.

4. Concluding remarks

One of the main objectives in this study is to show the similarity between the theoretical and observational energy spectral peaks for planetary waves. The equivalent height, h_m, represents the vertical scale of motions, and the eigenfrequency of Laplace's tidal equations, σ_{nlm}, measures the 3-D scale of motions due to the intrinsic dispersion relation of Rossby waves.

We found characteristic bimodal energy peaks in the vertical wavenumber domain at $h_m^{-1} = 1 \times 10^{-4}$ and 7×10^{-3} (m^{-1}). We also found a distinct energy peak in the eigenfrequency domain at $|\sigma_{nlm}| = 8 \times 10^{-2}$, which separates the 3 power law in the low-frequency range and -5/3 power law in the high-frequency range. The results were compared with the theoretically expected energy peaks due to atmospheric baroclinic instability on a sphere. It was confirmed that the baroclinic instability of shallow Charney modes has the expected structure; i.e., characteristic bimodal energy peaks in the vertical wavenumber domain and a distinct energy peak in the eigenfrequency domain. It is understandable for wavenumber 6 that the observed energy peaks in these spectral domain are resulted from the atmospheric baroclinic instability on a sphere. In the real atmosphere, the supplied energy would cascades away from the source range toward the rest of the spectral domain through the nonlinear scattering.

Contrasted with the reasonable interpretation of energy peaks for wavenumber 6, the interpretation of the energy peaks in planetary waves has been less clear in previous research. We found that the slow Charney modes and the dipole Charney modes in planetary waves exhibit the anticipated bimodal energy peaks in the vertical wavenumber domain and a sharp energy peak in the eigenfrequency domain. The resulting energy source due to atmospheric baroclinic instability coincides with the observed energy peaks of planetary waves in the eigenfrequency domain in a manner similar to synoptic waves. The results suggest that low-frequency unstable planetary waves contribute a substantial fraction of the energy peaks in the eigenfrequency domain.

The time-mean structure of planetary waves is not the steady solution, but a statistical average of episodic amplifications of transient planetary waves. The structures of the low-frequency unstable planetary waves are very similar to the linear steady solutions. The present study provides an alternative interpretation of the time-mean vertical structures of planetary waves as the occasional amplification of the low-frequency unstable planetary waves

Because low-frequency unstable planetary waves are free modes, they are more likely to be excited resonantly by many additional external forcing than would neutral free Rossby waves. Additional quasi-stationary forcing or transient forcing tends to excite the low-frequency unstable modes selectively from other numerous normal mode.

Acknowledgments This research was supported by the National Science Foundation under Grant ATM-8923064.

References

Kasahara, A., and H. L. Tanaka, 1989: Application of vertical normal mode expansion to problems of baroclinic instability. *J. Atmos. Sci.*, **46**, 489-510.

Kraichnan, R. H., 1967: Inertial range in two-dimensional turbulence. *Phys. Fluids*, **10**, 1417-1423.

Leith, C. E., 1968: Diffusion approximation for two-dimensional turbulence. *Phys. Fluids*, **11**, 671-672.

Lilly, D. K., 1989: Two-dimensional turbulence generated by energy sources at two scales. *J. Atmos. Sci*, **46**, 2026-2030.

Shepherd, T. G., 1987. A spectral view of nonlinear fluxes and stationary-transient interaction in the atmosphere. *J. Atmos. Sci.*, **44**, 1166-1178.

Tanaka, H. 1985. Global energetics analysis by expansion into three-dimensional normal mode functions during the FGGE winter. *J. Meteor. Soc. Japan*, **63**, 180-200.

Tanaka, H. L., and E. C. Kung, 1988: Normal mode energetics of the general circulation during the FGGE year. *J. Atmos. Sci.*, **45**, 3723-3736.

Tanaka, H. L., and E. C. Kung, 1989: A study of low-frequency unstable planetary waves in realistic zonal and zonally varying basic states. *Tellus*, **41A**, 179-199.

Tanaka, H. L., and S. Sun, 1990: A study of baroclinic energy source for large-scale atmospheric normal modes. *J. Atmos. Sci.*, **47**, 2674-2695.

Young, R. E., and G. L. Villere, 1985: Nonlinear forcing of planetary scale waves by amplifying unstable baroclinic eddies. *J. Atmos. Sci.*, **42**, 1991-2006.